CROATICA CHEMICA ACTA CCACAA **70** (1) 55–69 (1997)

ISSN-0011-1643
CCA-2406

Original Scientific Paper

Application of the Pitzer Model to Solar Salt Brine Chemistry*

Vesna Vančina,[a] *Dana R. Kester,*[b] *and Halka Bilinski*[c]

[a]*University of Zagreb, Faculty of Graphic Arts, P.O.B. 225, 10001 Zagreb, Croatia,*

[b]*University of Rhode Island, Graduate School of Oceanography, Narragansett, RI 02882 USA*

[c]*Ruđer Bošković Institute, Department of Chemistry, P.O.B. 1016, 10001 Zagreb, Croatia*

Received January 18, 1996; accepted June 6, 1996

A series of liqiud samples from the Seča solar saltwork was collected and analyzed for the major ions along with Adriatic seawater. The most concentrated saltwork brine was further evaporated in the laboratory. These samples provided a set of solutions ranging from 0.7 to 13.6 ionic strength (in molality), from which various solid phases precipitated during the evaporation. A Pitzer model for ionic activity coefficients was used to calculate the ion activity products of various phases in these solutions. The composition of the evaporation brines was controlled by the *K*s of gypsum, anhydrite, halite, epsomite, and possibly astrakhainite over various ionic strength ranges.

INTRODUCTION

Sodium chloride and other salts are among the most valuable chemical resources extracted from seawater on the global basis. Solar saltworks have a widespread distribution around the world, especially at latitudes of less than about 45 degrees, where the climatic conditions are favourable for the

* Dedicated to Marko Branica on the occasion of his 65th birthay.

evaporation of seawater to highly concentrated brines. Economic success of a solar sea salt operation depends on the efficiency of the production and the quality of the product. An understanding of the chemistry that occurs in these systems will help achieve a successful operation.[1–3]

We have been investigating the chemistry of brines at the solar saltwork at Seča, Slovenia in the northern Adriatic Sea. In this, and most other marine solar saltworks, seawater is brought into a set of ponds and allowed to evaporate. The evaporation process is monitored by measuring a property such as density, and when the density reaches certain levels the brine is moved progressively through a set of ponds. At certain densities, specific types of salts will precipitate and crystallize from the brine. When most of the desired salt is precipitated, the brine is moved to subsequent ponds or discharged to the sea. The salt can be recovered from the bottom of the pond, washed, and processed for its commercial use.[4–6]

There are many geochemically and commercially significant evaporite deposits around the world in which large volumes of seawater have evaporated over a period of time resulting in massive salt deposits of halite, gypsum, anhydrite, and epsomite. Studies of the chemistry of solar saltworks provide an insight into the conditions which are likely to have prevailed when evaporite deposits were forming.[7,8]

There are also a number of environments where seawater is evaporated to very high concentrations, leading to the formation of salt phases on small scales. One example of such localized evaporation is in tide pools where seawater can be trapped long enough for extensive evaporation and crystallization processes to occur. Another example is in seawater droplets that are injected into the atmosphere and which undergo evaporation to produce sea salt aerosols.

In this study, a set of brine samples of various densities was collected. Further evaporation was performed in the laboratory to obtain a fairly complete progression of evaporation brines.

The objectives of this study were to use analytical information on brine composition[9,10] to determine the sequences of solid phases that form from the brines of various densities, and to examine a solubility model of the degree of saturation of the brines with respect to major salt solid phases. The aqueous solutions in this study covered an ionic strength (I) ranging from the incoming Adriatic seawater (I = 0.711) to I = 13.58 for the most concentrated brine. Ionic strength is given in molality.

Pitzer and coworkers published a series of papers presenting a set of equations and coefficients which are very effective for calculating the thermodynamic properties of multicomponent electrolyte solutions from experimental data on single salt solutions and on binary and ternary mixtures of salts.[11–15]

This model is able to fit the experimental data to high concentrations such as 6 molal for NaCl and 3 molal for $MgSO_4$. Other workers have applied this model to geochemical systems for the prediction of mineral solubilities in various aqueous solutions.[16–22] A recent review of the Pitzer model was provided by Pitzer[23] while its application to natural waters was presented by Clegg and Whitfield[24] and Pabalan and Pitzer.[25]

We used the Pitzer model of activity coefficients γ in multicomponent electrolyte solutions[26] to compute the ion activity products of potentially important solid phases.

The Pitzer equations used to calculate ionic activity coefficients in multicomponent electrolyte solutions have been given in many papers as well as recent reviews.[23–25] We have used the formulation and notation given by Harvie and Weare.[16]

For the cations, M:

$$\ln \gamma_M = z_M^2 F + \sum_a m_a (2B_{Ma} + ZC_{Ma}) + \sum_c m_c \left(2\Phi_{Mc} + \sum_a m_a \Psi_{Mca}\right) + \\ + \sum_{a<a'} \sum m_a m_{a'} \Psi_{aa'M} + |z_M| \sum_c \sum_a m_c m_a C_{ca}$$

For the anions, X:

$$\ln \gamma_X = z_X^2 F + \sum_c m_c (2B_{cX} + ZC_{cX}) + \sum_a m_a \left(2\Phi_{Xa} + \sum_c m_c \Psi_{Xac}\right) + \\ + \sum_{c<c'} \sum m_c m_{c'} \Psi_{cc'X} + |z_X| \sum_c \sum_a m_c m_a C_{ca} .$$

In these equations, m_i is the molality of the I ions, with M, c, and c' referring to cations, and X, a and a' referring to anions. The double summations over c < c' and a < a' are for interactions of pairs of dissimilar like-charged ions.

The term Z is given by $Z = \sum_i |z_i| m_i$, and the term F is given by:

$$F = -A^\Phi \left[\sqrt{I} / \left(1 + b\sqrt{I}\right) + (2/b) \ln\left(1 + b\sqrt{I}\right) \right] + \sum_c \sum_a m_c m_a B'_{ca} + \\ + \sum_{c<c'} \sum m_c m_{c'} \Phi'_{cc'} + \sum_{a<a'} \sum m_a m_{a'} \Phi'_{aa'}$$

in which I is the ionic strength, $I = \frac{1}{2} \sum z_i^2 m_i$, and b is assigned a value of 1.2 for all electrolytes.

The term A^{Φ} is given by:

$$A^{\Phi} = 1/3\ (2\pi\ N_0\ \rho_w/1000)^{1/2}\ [e^2/DkT)]^{3/2},$$

with N_0 being Avogadro's number, ρ_w is the density of water, e is the charge of an electron, D is the dielectric constant of pure water, k is the Boltzmann constant, and T is absolute temperature.

Variables B and C are given by the following expressions:

For electrolytes in which one or both ions are univalent

$$B_{MX} = \beta^0{}_{MX} + \beta^1{}_{MX}\, g\ (\alpha\sqrt{I})$$

$$B'_{MX} = \beta^1{}_{MX}\, g'\ (\alpha\sqrt{I})\ /\ I$$

and α is assigned a value of 2. For electrolytes that are 2:2 or higher valence types

$$B_{MX} = \beta^0{}_{MX} + \beta^1{}_{MX}\, g\ (\alpha_1\sqrt{I}) + \beta^2{}_{MX}\, g\ (\alpha_2/\sqrt{I})$$

$$B'_{MX} = \beta^1{}_{MX}\, g'\ (\alpha_1\sqrt{I})\ /\ I + \beta^2{}_{MX}\, g'\ (\alpha_2/\sqrt{I})\ /\ I.$$

For 2:2 electrolytes $\alpha_1 = 1.4$ and $\alpha_2 = 12.\dot{0}$.

Functions g and g' have the following form:

$$g(x) = 2[1 - (1 + x)e^{-x}]\ /\ x^2$$

$$g'(x) = -2[1 - (1 + x + (1/2)x^2)e^{-x}]\ /\ x^2$$

with $x = \alpha\sqrt{I}$.

C_{MX} is given by:

$$C_{MX} = C^{\Phi}{}_{MX}\ (2\,|\,z_M\, z_X\,|^{1/2})\ .$$

Coefficients $\beta^0{}_{MX}$, $\beta^1{}_{MX}$, $\beta^2{}_{MX}$, and $C^{\Phi}{}_{MX}$ are obtained from osmotic and activity coefficient data in single salt solutions of each electrolyte MX. The higher order terms for cation-cation and anion-anion interactions are obtained from the data in aqueous solutions of two electrolytes which provide values for the Φ parameters. Two-salt aqueous solutions also provide the basis for obtaining the Ψ parameters which account for cation-cation-anion and anion-anion-cation interactions. Details by which these higher order interaction terms are evaluated are given by several workers.[15,16,18,23–25]

EXPERIMENTAL

Chemicals and Samples

The following reagent grade chemicals were used in this work for the analysis of macroconstituents and preparation of artificial seawater:[27] $AgNO_3$, $BaCl_2 \cdot 2H_2O$, $CaCO_3$, Calcon, Eriochrome Black T (EBT), di-sodium salt of ethylenediamine-N,N,N',N',-tetra-acetic acid (EDTA), H_3BO_3, HCOONa, HCl, H_2SO_4, HCOONa, KBr, KCl, K_2CrO_4, KI, Methyl Orange, Methyl Red, $MgCl_2 \cdot 6H_2O$, NaCl, NaOH, $Na_2S_2O_3$, NaF, Na_2SO_4, NH_4Cl, NH_4OH, $(NH_4)_6Mo_7O_{24}$, starch and $SrCl_2 \cdot 6H_2O$ (Merck, Darmstadt, Germany).

Three types of liquid samples were obtained: *incoming seawater*, Adriatic seawater entering the solar saltworks Seča (Sample 1, Table I); *brines* (concentrated seawater) of various densities from solar evaporation, lime, pickle and crystallizing or harvesting ponds of the saltwork Seča (Samples 2–10, Table I); and *laboratory brines* (Samples 11–17, Table I) obtained by isothermal laboratory evaporation of Sample 10, Table I.

Samples collected at the solar saltwork were centrifuged to remove suspended particles prior to the density measurement by pycnometer at 25 °C and chemical analysis of macroconstituents of importance for the solar salt production.

Instrumentation and Analysis

Sodium and potassium were determined by atomic absorption spectrophotometry using a Perkin Elmer 5000 instrument. The sum of calcium and magnesium was determined by an EDTA complexometric titration at pH 10, and calcium was measured by an EDTA complexometric titration at pH 12.5; magnesium was determined by difference. Chloride was determined by a modified Mohr's titration and bromide by titration with $Na_2S_2O_3$. Sulfate was determined gravimetrically as $BaSO_4$.[28,29]

Procedure Used in Laboratory Evaporation Experiments

The temperature in the laboratory was 20 ± 3 °C and the relative humidity approximately 60–80%.

Seven 2000 ml beakers were filled with centrifuged Sample 10, Table I. The beakers were heated on a water bath at 25 ± 1 °C. A ventilator was used to move air across the beakers at a speed of 1 m s^{-1}.

Evaporation of brines was conducted every day from 8 a.m. to 5 p.m., after which time the thermostated water bath and ventilator were switched off. The quiescent period during the night was similar to the conditions that exist at the solar saltwork.

Evaporation was conducted until the desired density of brine in each beaker was reached (this was easily controlled by the so called specific volume »*y*«[30]) and then the liquid phase was immediately separated from the solid phase.

The density of each laboratory brine (Samples 11–17, Table I) was determined by pycnometer at 25 °C and then laboratory brines were diluted and analyzed for macroconstituents.

RESULTS AND DISCUSSION

The densities and chemical data of macrocomponents in liquid samples are summarized in Table I together with the ionic strength in molality.

We used the Pitzer model of electrolyte solution thermodynamics to calculate the activity coefficients γ and the activity of major ions as well as the activity of water in the liquid samples. Results of these calculations are summarized in Table II.

In this study, we used the database and algorithm for the Pitzer model developed by Plummer *et al.*[26] For multicomponent solutions, such as seawater and its brines, it is most convenient to partition electrolyte activity coefficients into a contribution attributable to the cation and a contribution attributable to the anion. This partitioning into individual ionic activity coefficients requires a non-thermodynamic convention. When these ionic activity coefficients, or activities are combined to calculate the mean ionic activity coefficients, ion activity products related to solid phases, or equilibrium constants in general, the non-thermodynamic assumptions used to arrive at the ionic activity coefficients cancel out, and one obtains valid estimates of solute activities. In Table III, we show the Ion Activity Products (IAP) for various combinations of cations and anions which may precipitate to form specific solid phases during the evaporation of seawater.

All of our calculations using the Pitzer model were done for a temperature of 25 °C. The analytical data for the liquid samples (seawater and brine solutions, Table I) show that the calcium concentration increases from Sample 1 (seawater) to Sample 4 (brine), and then decreases to Sample 10 (brine). Calcium can form three principal insoluble phases in these brines: calcite ($CaCO_3$), gypsum ($CaSO_4 \cdot 2H_2O$) and anhydrite ($CaSO_4$).[1,2,4]

Figure 1 shows the variation in the IAP = $a\text{Ca} \cdot a\text{SO}_4 \cdot (a\text{H}_2\text{O})^2$ in the sequence of brine solutions. Also shown in this figure is the value for the *K*s for gypsum. The composition of evaporated seawater brine reaches saturation with repect to gypsum at an ionic strength of about 2.3 (Sample 4, Table I); the composition remains virtually fixed at this IAP over the ionc strength range of 2.3 to 8.4 as calcium is removed from the aqueous (liquid) phase by precipitation and crystallization.

Figure 2 shows the IAP for $a\text{Ca} \cdot a\text{SO}_4$ and its relationship to the *K*s for anhydrite. Samples (brines) with ionic strengths between 6.8 and 8.4 are near saturation with respect to anhydrite.

The IAP-*K*s relationship for halite (NaCl) is shown in Figure 3. The results suggest that the brines became supersaturated with respect to halite in Sample 9 (brine) and precipitation then occurs with further evaporation. This set of Samples 11–17 (brines) were produced during the laboratory evaporation experiments rather than in the solar saltwork ponds. Kinetic

TABLE I

Density, major ion molarity and molality, and calculated ionic strength in molality of liquid samples

Sample	$\rho_{meas.}$	$[Ca]_{tot.}$	$m(Ca)$	$[Mg]_{tot.}$	$m(Mg)$	$[Na]_{tot.}$	$m(Na)$	$[K]_{tot.}$	$m(K)$	$[Cl]_{tot.}$	$m(Cl)$	$[SO_4]_{tot.}$	$m(SO_4)$	$[Br]_{tot.}$	$m(Br)$	I
1	1.0255	0.011	0.011	0.055	0.056	0.468	0.474	0.010	0.010	0.549	0.555	0.029	0.029	0.0009	0.001	0.711
2	1.0420	0.017	0.017	0.091	0.092	0.762	0.774	0.016	0.016	0.897	0.913	0.047	0.048	0.0014	0.001	1.166
3	1.0755	0.026	0.027	0.178	0.184	1.425	1.473	0.027	0.028	1.674	1.731	0.092	0.095	0.0026	0.003	2.228
4	1.0813	0.033	0,034	0.183	0.189	1.486	1.534	0.031	0.032	1.753	1.815	0.095	0.098	0.0030	0.003	2.332
5	1.1124	0.030	0.032	0.267	0.280	2.145	2.253	0.044	0.046	2.533	2.666	0.121	0.127	0.0040	0.004	3.360
6	1.1435	0.024	0.026	0.351	0.377	2.892	3.109	0.061	0.066	3.406	3.669	0.145	0.156	0.0053	0.006	4.540
7	1.1712	0.015	0.016	0.438	0.480	3.529	3.868	0.066	0.072	4.156	4.557	0.170	0.186	0.0063	0.007	5.613
8	1.2055	0.012	0.013	0.536	0.597	4.170	4.645	0.079	0.088	4.926	5.494	0.205	0.228	0.0077	0.009	6.788
9	1.2304	0.005	0.006	0.916	1.034	4.063	4.587	0.133	0.150	5.320	6.017	0.352	0.397	0.0120	0.014	8.251
10	1.2322	0.005	0.006	0.995	1.122	3.941	4.445	0.135	0.152	5.301	5.995	0.380	0.429	0.0128	0.014	8.410
11	1.2582	–	–	1.760	2.018	3.118	3.575	0.220	0.252	5.534	6.367	0.681	0.781	0.0182	0.021	10.695
12	1.2634	–	–	1.925	2.171	2.699	3.044	0.245	0.275	5.272	5.969	0.727	0.819	0.0200	0.023	10.626
13	1.2652	–	–	1.983	2.229	2.594	2.917	0.258	0.290	5.196	5.869	0.755	0.850	0.0206	0.023	10.698
14	1.2794	–	–	2.350	2.631	1.869	2.093	0.309	0.346	5.242	5.899	0.897	1.005	0.0265	0.030	11.439
15	1.2936	–	–	2.759	3.115	1.524	1.721	0.349	0.393	5.354	6.085	1.038	1.172	0.0340	0.038	12.674
16	1.2978	–	–	3.029	3.443	1.312	1.491	0.403	0.459	5.651	6.464	0.992	1.128	0.0366	0.042	13.349
17	1.3031	–	–	3.178	3.608	1.091	1.239	0.425	0.482	5.964	6.816	0.923	1.049	0.0402	0.046	13.580

Concentrations are in molar $[\ ]_{tot}$ determined and in molal m ( ) units calculated;
– not determined

TABLE II

The »conventional« ionic activity coefficients γ, activity of major ions and water in the liquid samples

Sample	$\gamma\ Ca^{2+}$	$a\ Ca^{2+}$	$\gamma\ Mg^{2+}$	$a\ Mg^{2+}$	$\gamma\ Na^{+}$	$a\ Na^{+}$	$\gamma\ K^{+}$	$a\ K^{+}$	$\gamma\ Cl^{-}$	$a\ Cl^{-}$	$\gamma\ SO_4^{2-}$	$a\ SO_4^{2-}$	$\gamma\ Br^{-}$	$a\ Br^{-}$	$a\ H_2O$
1	0.187	0.0021	0.205	0.0115	0.638	0.3016	0.589	0.0059	0.691	0.3829	0.107	0.0031	0.717	0.0007	0.9817
2	0.174	0.0030	0.198	0.0182	0.616	0.4767	0.545	0.0087	0.687	0.6259	0.077	0.0037	0.727	0.0007	0.9697
3	0.183	0.0050	0.226	0.0416	0.610	0.8982	0.491	0.0137	0.723	1.2503	0.048	0.0045	0.803	0.0024	0.9399
4	0.186	0.0063	0.231	0.0436	0.611	0.9375	0.487	0.0156	0.729	1.3203	0.046	0.0045	0.814	0.0024	0.9369
5	0.235	0.0075	0.315	0.0883	0.641	1.4438	0.462	0.0212	0.799	2.1269	0.035	0.0044	0.936	0.0037	0.9029
6	0.337	0.0088	0.497	0.1874	0.699	2.1752	0.445	0.0294	0.907	3.3211	0.028	0.0044	1.122	0.0067	0.8590
7	0.481	0.0077	0.778	0.3735	0.768	2.9714	0.433	0.0312	1.038	4.7307	0.025	0.0046	1.353	0.0095	0.8161
8	0.706	0.0092	1.269	0.7574	0.855	3.9702	0.420	0.0369	1.219	6.6846	0.023	0.0052	1.683	0.0151	0.7677
9	0.760	0.0046	1.595	1.6487	0.883	4.0509	0.373	0.0559	1.587	9.5289	0.025	0.0100	2.378	0.0333	0.7273
10	0.727	0.0044	1.554	1.7433	0.874	3.8861	0.364	0.0554	1.649	9.8594	0.026	0.0112	2.496	0.0349	0.7257
11	–	–	1.837	3.7102	0.871	3.1133	0.287	0.0724	2.622	16.6410	0.034	0.0268	4.477	0.0940	0.6742
12	–	–	1.379	2.9937	0.813	2.4736	0.277	0.0763	2.726	16.2090	0.037	0.0307	4.642	0.1068	0.6895
13	–	–	1.281	2.8596	0.798	2.3293	0.272	0.0789	2.794	16.3330	0.039	0.0327	4.774	0.1098	0.6916
14	–	–	1.317	3.4660	0.786	1.6454	0.249	0.0862	3.271	19.1970	0.043	0.0435	5.686	0.1706	0.6811
15	–	–	1.458	4.5451	0.790	1.3589	0.218	0.0859	4.357	26.3370	0.053	0.0617	8.024	0.3049	0.6488
16	–	–	1.720	5.9249	0.810	1.2078	0.201	0.0920	5.406	34.7250	0.061	0.0689	10.428	0.4380	0.6194
17	–	–	2.059	7.4336	0.834	1.0335	0.195	0.0939	5.941	40.2280	0.065	0.0680	11.609	0.5340	0.6022

– not determined

TABLE III

Solid phase log *Ks* at 25 °C and the log IAP values in the liquid samples

Sample	GYPSUM $CaSO_4 \cdot 2H_2O$	ANHYDRITE $CaSO_4$	HALITE NaCl	ASTRAKHAINITE $Na2SO_4 \cdot MgSO_4 \cdot 4H_2O$	EPSOMITE $MgSO_4 \cdot 7H_2O$
1	–5.210	–5.194	–0.938	–8.030	–4–505
2	–4.989	–4.963	–0.525	–7.305	–4.268
3	–4.702	–4.649	0.050	–6.269	–3.913
4	–4.601	–4.544	0.093	–6.220	–3.904
5	–4.566	–4.477	0.487	–5–619	–3.718
6	–4.548	–4.416	0.859	–5.033	–3.548
7	–4.626	–4.449	1.148	–4.506	–3.381
8	–4.547	–4.317	1.424	–3.942	–3.204
9	–4.618	–4.341	1.587	–3.120	–2.751
10	–4.591	–4.313	1.583	–3.042	–2.686
11	–	–	1.714	–2.272	–2.201
12	–	–	1.603	–2.409	–2.167
13	–	–	1.580	–2.420	–2.150
14	–	–	1.500	–2.418	–1989
15	–	–	1.554	–2.247	–1.868
16	–	–	1.623	–2.219	–1.845
17	–	–	1.619	–2.316	–1.838
log *Ks*	–4.581	–4.362	1.570	–2.347	–1.881
Ksp =	$a_{Ca}\, a_{SO_4}\, a^2_{SO_4}$	$a_{Ca}\, a_{SO_4}$	$a_{Na}\, a_{Cl}$	$a^2_{Na}\, a_{Mg}\, a^2_{SO_4}\, a^4_{H_2O}$	$a_{Mg}\, a_{SO_4}\, a^7_{H_2O}$

factors, such as the rate of evaporation, may be important in the halite supersaturation phenomenon.

A plot of Na^+ molality *vs.* ionic strength in Figure 4 shows a maximum plateau in brines 8 and 9 with a decrease from brines 9 to 11, and a sharp drop in brines 11 to 14. For Cl^- (Figure 4) molality increases up to brine 11 and then there is a sharp drop for brines 11 to 13 as halite begins to precipitate. These results imply that a phase precipitates from brine 9 to 11 (ionic strengths 8.2 to 10.7) that contains Na^+ but not Cl^-. Similar bahaviour is described by Garrett.[4]

In Figure 5, the IAP-*Ks* relationship is shown for astrakhainite ($Na_2SO_4 \cdot MgSO_4 \cdot 4H_2O$). The calculation shows its possible coprecipitation with halite starting from sample 11 (laboratory brine).

Figure 6 shows the IAP-*Ks* relationship for epsomite ($MgSO_4 \cdot 7H_2O$). The brines become progressively more saturated with respect to epsomite until saturation is reached with brine 15, and the composition then remains near the *Ks* for this phase. In brines 15, 16 and 17, the Mg^{2+} molality increases steadily from 3.1 to 3.6, while the SO_4^{2-} molality decreases from 1.172 to 1.048.

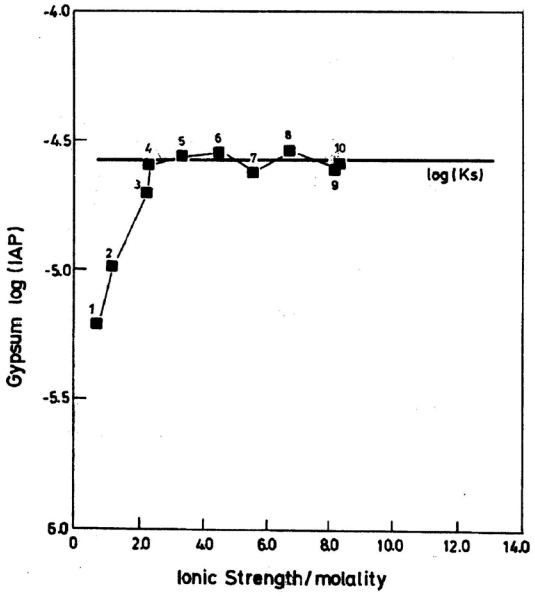

Figure 1. Variation in the Ion Activity Product (IAP) for gypsum in the saltwork brine solutions as a function of ionic strength. The horizontal line shows the value for the *K*s of gypsum at 25 °C. The number near each symbol refers to the sample number in Table I.

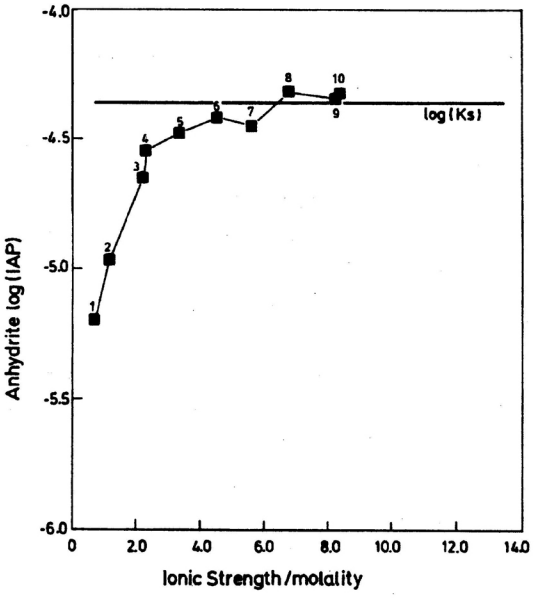

Figure 2. Variation in the Ion Activity Product (IAP) for anhydritre, with its *K*s, in the same format as Figure 1.

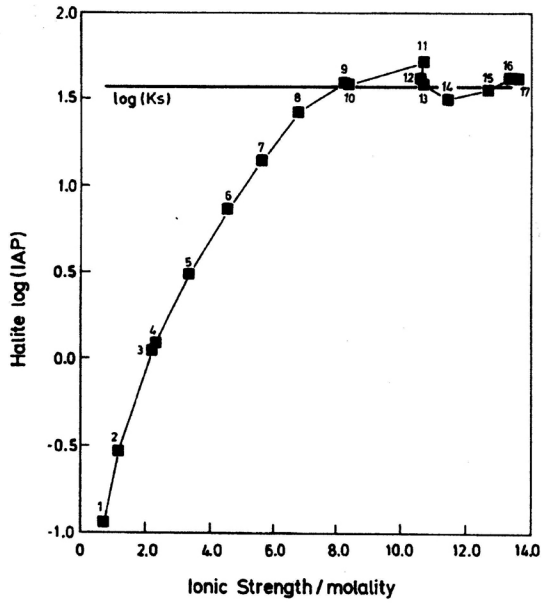

Figure 3. Variation in the Ion Activity Product (IAP) for halite, with its *K*s, in the same format as Figure 1.

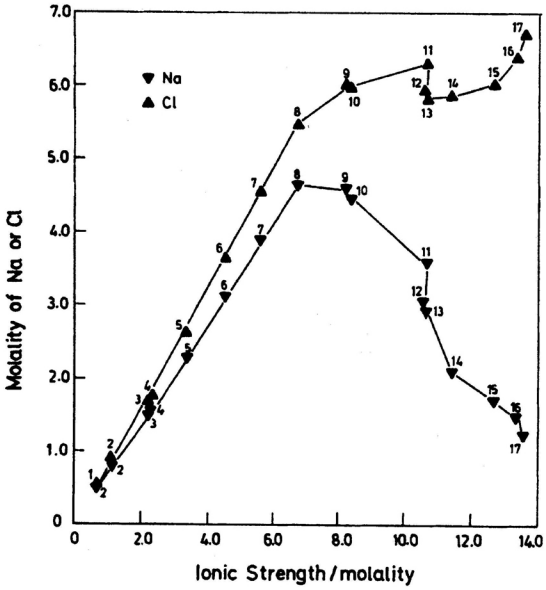

Figure 4. The molality of chloride and sodium ions in the seawater and in the brine solutions as a function of the ionic strength. The number near each symbol refers to sample numbers in Table I.

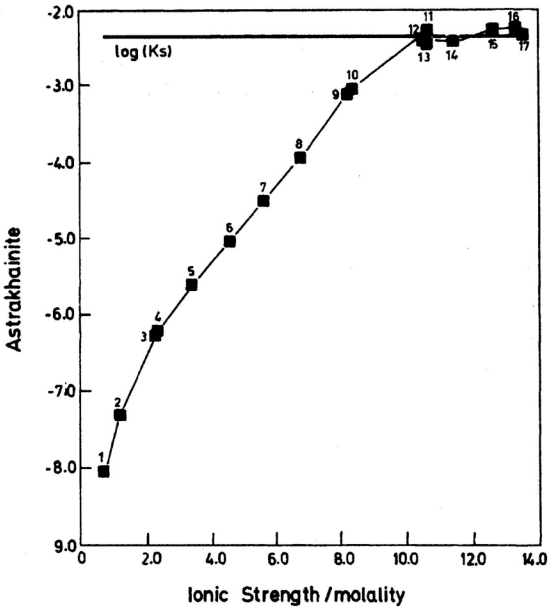

Figure 5. Variation in the Ion Activity Product (IAP) for astrakhainite, with its *K*s, in the same format as Figure 1.

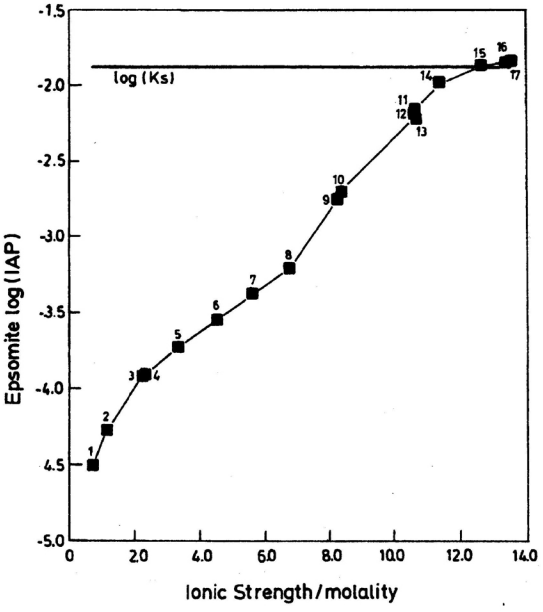

Figure 6. Variation in the Ion Activity Product (IAP) for epsomite, with its *K*s, in the same format as Figure 1.

TABLE IV

Summary of the degree of saturation of the liquid samples with respect to various solid phases

Solid phase	Ionic Strength Range	Degree of Saturation Mean (%)	Std. dev. (%)
Gypsum $CaSO_4 \cdot 2H_2O$	2.3–8.4	99	7
Anhydrite $CaSO_4$	6.7–8.4	109	3
Halite NaCl	8.2–13.6	107	14
Astrakhainite $Na_2SO_4 \cdot MgSO_4 \cdot 4H_2O$	10.7–13.6	104	19
Epsomite $MgSO_4 \cdot 7H_2O$	12.6–13.6	107	3

Column 2 is the ionic strength range over which IAP reached a plateau in Figures I, II, III, V and VI. Columns 3 and 4 are the mean and standard deviation of the degree of saturation in the brines over that ionic strength range.

Comparisions of ion activity products and solubility products for five solid phases are summarized in Table IV. Once the brine solutions reach a plateau composition for these five solid phases, they are very close to equlibrium with the solubility product of these phases. These results indicate that the Pitzer model, when applied to concentrated seawater brines, provides ion activity products that are within 5–10% of the *K*s values for the phases that are likely to control the brine composition. This quantitative agreement holds for very high ionic strengths, up to 13.6 on a molal scale. The brines in this study did not reach the *K*s for arcanite (K_2SO_4), bischofite ($MgCl_2 \cdot 6H_2O$), carnallite ($KCl \cdot MgCl_2 \cdot 6H_2O$), glauberite ($Na_2SO_4 \cdot Ca(SO_4)_2$), or sylvite (KCl).

CONCLUSIONS

Combining the Pitzer model with the analytical data for the major ions in seawater evaporation brines provides a valuable insight into the thermodynamic conditions in these very concentrated aqueous solutions. A remarkably good correspondence was found between the aqueous phase ion activity products for gypsum, anhydrite, halite, astrakhainite and epsomite and the well-established thermodynamic solubility products for these phases.

*Experimental part of this work is from Ph. D. Dissertation of V. Vančina (1990).

Acknowledgement. – The work was supported by the Ministry of Science and Technology of the Republic of Croatia; Project no. 00980606.

REFERENCES

1. W. F. McIlhenny, *Extraction of Economic Inorganic Materials from Sea Water*, in: J. P. Riley and G. Skirrow (Eds.), *Chemical Oceanography*, Vol 4, Academic Press, London, 1975, pp. 155–214.
2. United Nations Industrial Development Organization, *Extraction of Chemicals from Seawater*, United Nation Publication ID/73, Sales No. E.71.II.B.25, Vienna, 1972, p. 59.
3. U. Petersen, Mininig the Hydrosphere, *Geochim. Cosmochim. Acta* **58** (1994) 2387–2403.
4. D. E. Garrett, *By-Products Recovery from Solar Salt Operations*, in: J. L. Rau (Ed.), Fifth Symposium on Salt, Vol 2, The Northern Ohio Geological Society, Cleveland, 1980, pp. 281–293.
5. H. Bauschlicher and W. Whlk, *Production of Vacuum Salt Based on Seawater as Raw Material*, in: B. C. Schreider and H. L. Harner (Eds.), Sixth International Symposium on Salt, Vol 2, The Salt Institute, Alexandria, 1983, pp. 495–452.
6. P. Jongema, *Production of Low Bromine-Containing Evaporated Salt*, in: H. Kakihana, H. R. Hardy, T. Hoshi and K. Toyokura (Eds.), Seventh Symposium on Salt, Elsevier, Amsterdam, 1993, pp. 159–163.
7. V. S. Hall and M. R. Spencer, *Salt, Evaporites and Brines*: An Annotated Bibliography, Oryx Press, Phoenix, 1984, p. 216.
8. P. Sonnenfeld, *Brines and Evaporites*, Academic Press, 1984, Orlando, p.613.
9. V. Vančina, *Precipitation of Various Salts from Salt Work Brines*, Ph. D. Dissertation, University of Zagreb, Faculty of Technology, Zagreb, Croatia, 1990, p 142.
10. V. Vančina and H. Bilinski, *Distribution of Macro- and Microconstituents between Brines and Sediments of the Solar Salt Work Seča*, Poster, International Symposia »Chemistry of the Mediterranean«, Rovinj, Croatia, May 11–18, 1994.
11. K. S. Pitzer, *J. Phys. Chem.* **77** (1973) 268–277.
12. K. S. Pitzer and G. Mayorga, *J. Phys. Chem.* **77** (1973) 2300–2308.
13. K. S. Pitzer and G. Mayorga, *J. Solution Chem.* **3** (1974) 539–546.
14. K. S. Pitzer and J. J. Kim, *J. Amer. Chem. Soc.* **96** (1974) 5701–5707.
15. K. S. Pitzer, *J. Solution Chem.* **4** (1975) 249–265.
16. C. E. Harvie and J. H. Weare, *Gochim. Cosochim. Acta* **44** (1980) 981–997.
17. C. E. Harvie, N. Moller, and J. H. Weare, *Gochim. Cosochim. Acta* **48** (1984) 723–751.
18. A. R. Felmy and J. H. Weare, *Geochim. Cosmochim. Acta* **50** (1986) 2771–2783.
19. R. T. Pabalan and K. S. Pitzer, *Geochim. Cosmochim. Acta* **51** (1987) 2429–2443.
20. N. Moller, *Geochim. Cosmochim. Acta* **52** (1988) 821–837.
21. J. P. Greenberg and N. Moller, *Geochim. Cosmochim. Acta* **53** (1989) 2503–2518.
22. R. J. Spencer, N. Moller, and J. H. Weare, *Geochim. Cosmochim. Acta* **54** (1990) 575–590.
23. K. S. Pitzer, *Ion Interactions Approach: Theory and Data Correlation*, in: K. S. Pitzer (Ed.), *Activity Coefficients in Electrolyte Solutions*, CRC Press, Boca Raton, 1991, pp. 75–153.
24. S. L. Clegg and M. Whitfield, *Activity Coefficients in Natural Waters*, in: K. S. Pitzer (Ed.), *Activity Coefficients in Electrolyte Solutions*, CRC Press, Boca Raton, 1991, pp. 279–434.

25. R. T. Pabalan and K. S. Pitzer, *Mineral Solubilities in Electrolyte Solutions*, in: K. S. Pitzer (Ed.), *Activity Coefficients in Electrolyte Solutions*, CRC Press, Boca Raton, 1991, pp. 435–490.
26. L. N. Plummer, D. L. Parkhurst, G. W. Fleming, and S. A. Dunkle, A Computer Program Incorporating Pitzer's equations for Calculations of Geochemical Reactions in Brines, U. S. Geological Survey, Water- Resources Investigations Report 88–4153, Reston, Virginia, 1988.
27. D. R. Kester, I. W. Duedall, D. N. Connors and R. M. Pytkowicz, *Limnol. Oceanogr.* **12** (1967) 176–179.
28. J. P. Riley, *Analytical Chemistry of Sea Water*, in: J. P. Riley and G. Skirrow (Eds.), *Chemical Oceanography*, Vol 3, Academic Press, London, 1975, pp. 193–515.
29. K. Grasshoff, *Methods of Seawater Analysis*, Verlag Chemie, Weinheim, 1976, p. 317.
30. J. Usiglio, *Annalen der Chemie* **27** (1849) 92–107, 172–191.

SAŽETAK

Primjena Pitzerova modela na kemiju vode solarne solane

Vesna Vančina, Dana S. Kester i Halka Bilinski

Na solani Seča obavljeno je uzorkovanje tekućih uzoraka. Prikupljene su vode sa solane, od morske vode kojom započinje proizvodni postupak do luga (matičnice) iz kristalizacije. U prikupljenim uzorcima određeni su makroelementi. Lug najveće gustoće uporabljen je za laboratorijsko isparavanje. Na taj je način dobiven niz otopina ionske jakosti od 0,7 do 13,6 mol/L, iz kojih su se tijekom isparavanja taložile različite soli. Uporabljen je Pitzerov model za izračunavanje koeficijenata aktiviteta kako bi se izračunao ionski produkt aktiviteta različitih soli u ispitivanoim otopinama. Vrijedosti Ks gipsa, anhidrita, halita, epsomita i, vjerojatno, astrakainita određuju sastav lugova u različitim intervalima ionske jakosti.